Removal of methylene blue from aqueous solution by walnut carbon: optimization using response surface methodology

S. Hajati[a,*], M. Ghaedi[b,*], H. Mazaheri[b]

[a]*Department of Physics, Yasouj University, Yasouj 75918-74831, Iran, Tel./Fax: +98 7412223048; email: hajati@yu.ac.ir*
[b]*Chemistry Department, Yasouj University, Yasouj 75918-74831, Iran, Tel./Fax: +98 7412223048;*
emails: m_ghaedi@mail.yu.ac.ir (M. Ghaedi), hamed.mazaheri19@yahoo.com (H. Mazaheri)

ABSTRACT

In this study, carbon was easily made from walnut wood as a low-cost and non-toxic natural adsorbent. It was used to remove methylene blue rapidly from aqueous solutions. This adsorbent was re-used after heating. Boehm titration method, BET surface area measurement, FTIR, and pH determination at zero point of charge (pH_{ZPC}) were used to characterize this adsorbent. Response surface methodology was used to reduce the number of experiments and to optimize the experimental factors such as pH of solution, contact time, initial dye concentration, and adsorbent dosage. The optimal conditions for the dye removal were found to be 10, 2.0 min, 9.00 mg/L, and 0.250 g for pH, contact time, initial dye concentration, and adsorbent dosage, respectively. The rapid adsorption of the MB dye is an advantage of this adsorbent. Various isotherm models were used to fit the experimental equilibrium data. The results showed the suitability and applicability of Langmuir model. Kinetic models such as pseudo-first-order, pseudo-second-order, Elovich, and intraparticle diffusion models indicated that the second-order equation model controls the kinetic of the adsorption process.

Keywords: Adsorption; Methylene blue; Carbon; Kinetic; Thermodynamic; Walnut wood

1. Introduction

Industrial effluents contain dyes with large amounts of suspended organic solids [1]. Presence of such effluents in water could generate hazards to aquatic life by enhancing mutagenic and carcinogenic effects. Textile, paper, and printing activities are some sources of dye-containing wastewater [2–6]. Conventional wastewater treatment protocol based on physicochemical, chemical, and biological processes includes coagulation and flocculation [7], adsorption [8], ozonation [9], electrochemical techniques [10], biosorption [11,12], and fungal decolonization [13]. Among them, adsorption is widely used for large-scale biochemical, chemical, environmental recovery, and purification applications [14]. This technique benefits from simple design and ease of operation by efficient non-toxic and low-cost adsorbents. Characteristics and appropriate selection of the adsorbent are based on factors such as removal capacity, treatment cost, and operating conditions [15]. Chemical treatment and biodegradation procedure are based on expensive and complex processes that generate toxic byproducts.

*Corresponding authors.

Walnut is an agricultural tree that grows in different regions. The wood of this tree has a variety of uses, such as carpentry work and fuel. Moreover, the waste wood of walnut tree is largely available. After burning and putting it into a sealed container while keeping it cooled, the carbon is prepared (see below for more details) which means that this walnut carbon (WC) is very cost effective, energy effective, and a non-toxic material. All these characteristics of this carbon make it more suitable than commercial activated carbon for the removal of water pollution. On the other hand, methylene blue (MB), with complicated chemical structure, has high resistance to light and oxidizing agents. In addition, its removal based on biological treatment and chemical precipitation is not environmental friendly and has low efficiency [16].

Therefore, we were motivated to prepare walnut carbon as an alternative to expensive or toxic adsorbents for the removal of methylene blue (MB) from wastewater. BET surface area measurement, FTIR, pH determination at zero point of charge (pH_{ZPC}), and Boehm titration method were used to characterize this adsorbent. The number of experimental runs was reduced by applying central composite design (CCD) under response surface methodology (RSM). The experimental conditions, such as pH of solution, contact time, initial dye concentration, and adsorbent dosage as well as the dye removal percentage as response, were studied and optimized. The extent to which the experimental factors interact with each other was also investigated. The optimal conditions for the MB removal were found to be pH 10, contact time 2.0 min, initial dye concentration 9.0 mg/L, and adsorbent dosage 0.25 g.

Various isotherm models, such as Langmuir, Freundlich, Tempkin, and Dubinin–Radushkevich were used to fit the experimental equilibrium data. The results showed the suitability and applicability of the Langmuir model. Kinetic models, such as pseudo-first-order, pseudo-second-order, Elovich and intra-particle diffusion models indicated that the pseudo-second-order model controls the kinetic of adsorption process. It was shown that the WC can be effectively used to remove the cationic dye of methylene blue from wastewater.

2. Experimental

2.1. Materials and instrumentation

Methylene blue with a CAS number 52.015, chemical formula $C_{16}H_{18}N_3SCl$ (MW = 319.86 g/mol), and λ_{max} of 664 nm was supplied by Sigma–Aldrich (M) SdnBhd, Malaysia and used as received. The stock solution (1,000 mg/l) of MB was prepared by dissolving 0.5 g of MB in 500-mL distilled water. All working solutions of the desired concentration were obtained by diluting the stock solution with distilled water. The concentration of MB in the solution was measured by analyzing the corresponding absorbance spectra (at 664 nm) acquired by a double beam UV–vis spectrophotometer (JASCO, Model UV–vis V-530, Japan). FTIR absorption spectra of selected samples before and after adsorption process were obtained using KBr discs on a FTIR 6300 in the region 4,000–400 cm^{-1}.

2.2. Preparation of WC

First, the walnut wood was chopped into small pieces (about 1 cm) and rinsed with distilled water. Then, the pieces were dried in an oven at a temperature of 105°C overnight. Afterwards, they were placed in a metal container with a small opening for the exhaust, and the container was heated with gas flame for one hour at a temperature above 400°C. The produced coal was then slowly cooled to room temperature. The product was washed again with distilled water. The WC was pulverized after drying and sieving with a mesh sieve 50, and then it was characterized by FTIR and pH determination at zero point of charge (pH_{ZPC}) by the pH drift method reported elsewhere [17].

Oxygen-containing functional groups were determined by the Boehm titration method [18]. WC of 1.000 g was kept in contact with 15-mL solution of $NaHCO_3$ (0.10 M), Na_2CO_3 (0.05 M), and NaOH (0.10 M) for acidic groups, and in contact with 15-mL solution of HCl (0.10 M) for basic groups at room temperature for more than two days. Subsequently, the aqueous solutions were back titrated with HCl (0.10 M) for acidic and with NaOH (0.10 M) for basic groups.

The number and type of acidic sites were calculated by considering that NaOH neutralizes carboxylic, lactonic, and phenolic groups, Na_2CO_3 neutralizes carboxylic and lactonic groups, and $NaHCO_3$ neutralizes only carboxylic groups. Carboxylic groups were, therefore, quantified by direct titration with $NaHCO_3$. The difference between the groups titrated with Na_2CO_3 and those titrated with $NaHCO_3$ was assumed to be lactones, as well as the difference between the groups titrated with NaOH and those titrated with Na_2CO_3 was assumed to be phenol. Basic sites were determined by titration with HCl. Neutralization points were known using pH indicators of phenolphthalein solution for the titration of strong base and strong acid. In order to neutralize basic groups/sites,

remaining HCl in the solution was back titrated with 0.1 M NaOH. The results for the characterization of the WC are presented in Table 1.

2.3. CCD and optimization of parameters

CCD is one of the most accepted experimental designs under RSM. This statistical technique was used to study the individual and synergetic effects of four factors, including pH of solution, amount of adsorbent, concentration of MB, and contact time on the removal percentage of MB as response. Thirty-one experiments were designed and run at different conditions at room temperature. The number of runs was obtained according the relation $2^n + 2n + n_c$, where n is the number of factors (four factors) and n_c is the number of center points (seven replicates). Then the removal percentage of MB was calculated. Coded and uncoded factor values together with the response values are listed in Table 2.

The following quadratic equation as optimal model predictor was used to optimize and predict the response (Y) against the parameters

$$Y = b_0 + \sum_{i=1}^{4} b_i x_i + \sum_{i=1}^{4} b_{ii} x_i^2 + \sum_{i=1}^{3} \sum_{j=i+1}^{4} b_{ij} x_i x_j \tag{1}$$

where x_i, x_j are the coded values of the factors, and b_0, b_i, b_{ii}, and b_{ij} are the constant, linear, quadratic, and interaction coefficients, respectively. The analysis of variance (ANOVA), the coefficient of determination R^2, probability P-value (with 95% confidence level), and fisher's test were used to evaluate the statistical significance and the characteristics of the reliability of the analysis. All the parameters and experimental data were studied using a software MINITAB (version 16.0).

Significant and insignificant terms were determined and then the predictive model was obtained by rewriting Eq. (1) in terms of the significant factors.

Table 1
Summary report on characterization of walnut carbon

Summary report	
Surface area	Amount
Single point surface area at p/p° = 0.206	32.587 m/g
BET surface area:	31.908 m/g
Langmuir surface area:	42.770 m/g
t-Plot micropore area:	21.531 m/g
t-Plot external surface area:	10.376 m/g
BJH adsorption cumulative surface area of pores between 17.000 and 3,000.000 Å width:	3.585 m/g
BJH desorption cumulative surface area of pores between 17.000 and 3,000.000 Å width:	1.999 m/g
Pore volume	
Single point adsorption total pore volume of pores less than 1256.713 Å width at p/p° = 0.984:	0.029 cm/g
t-Plot micropore volume:	0.010 cm/g
BJH adsorption cumulative volume of pores between 17.000 and 3,000.000 Å width:	0.019 cm/g
BJH desorption cumulative volume of pores between 17.000 and 3,000.000 Å width:	0.013 cm/g
Pore size	
Adsorption average pore width (4 V/A by BET):	36.391 Å
BJH adsorption average pore width (4 V/A):	208.962 Å
BJH desorption average pore width (4 V/A):	265.473 Å
Nanoparticle size	
Average particle size:	1880.417 Å
pH Zero point of charge	
pH$_{ZPC}$	8.500
Solubility	
Acid soluble	NO
Water soluble	NO
Boehm titration	
Carboxylic(acidic functions)	0.875 mmol/g
Phenol	NO
Lactones	0.248 mmol/g
Basic sites	1.125 mmol/g

Table 2
CCD of the removal of MB by walnut carbon

Run	PH	Dye concentration (mg/L)	Time (min)	Adsorbent (g)	Removal (%)
1	2	10	20	0.225	88.410
2	8	14	11	0.325	89.540
3	6	10	20	0.225	87.540
4	6	10	20	0.225	91.340
5	8	14	29	0.325	93.830
6	6	10	20	0.425	98.330
7	6	10	20	0.225	92.710
8	4	14	29	0.125	55.920
9	8	6	29	0.125	88.390
10	4	6	29	0.325	98.140
11	8	6	11	0.125	85.070
12	6	10	20	0.225	91.120
13	6	10	20	0.025	18.610
14	4	14	11	0.125	51.620
15	8	6	11	0.325	98.330
16	8	6	29	0.325	98.540
17	4	14	11	0.325	92.270
18	4	6	11	0.325	97.530
19	8	14	11	0.125	50.120
20	6	10	20	0.225	95.760
21	6	10	2	0.225	83.310
22	6	10	38	0.225	93.690
23	4	14	29	0.325	94.710
24	8	14	29	0.125	55.510
25	6	10	20	0.225	87.110
26	10	10	20	0.225	93.920
27	6	18	20	0.225	62.680
28	6	10	20	0.225	86.130
29	4	6	29	0.125	87.260
30	6	2	20	0.225	92.220
31	4	6	11	0.125	82.740

$$Y = 90.24 + 30.48x_2 - 17.63x_3 - 29.39x_2^2 - 10.41x_3^2 + 27.03x_2x_3 \quad (2)$$

Positive coefficients mean that the corresponding terms affect the response positively, while the negative values affect it negatively. The terms x_2, x_3, x_2^2, x_3^2, and x_2x_3 stand for the amount of adsorbent, the dye concentration, the square of adsorbent amount, the square of dye concentration as well as the interaction of the adsorbent amount, and the dye concentration, respectively.

The ANOVA was performed and it showed that the *P*-values for the terms included in Eq. (2) are less than 0.05, and the *P*-value for lack of fit is higher than 0.05, indicating the adequacy and significance of the model. The terms x_2, x_3, x_2^2, x_3^2, and x_2x_3 were found to be significant. This shows the linear and quadratic responses of the MB removal against the MB concentration and the amount of WC. It also shows that the response is affected by the interaction of these two factors. Three-dimensional response surface for the significant factors is shown in Fig. 1.

The optimized values for the factors pH, the amount of WC, MB concentration, and contact time were found to be 10, 0.25 g, 9.0 mg/L, and 2.0 min, respectively. At this condition, the removal percentage of MB was predicted to be 96.60% with a desirability of 0.9509. The optimization plot was shown in Fig. 2. To make a test on the reliability of this prediction, an experiment was run at the obtained optimal condition and the removal percentage was obtained to be 94.20% which is very close to the predicted condition.

2.4. Adsorption studies

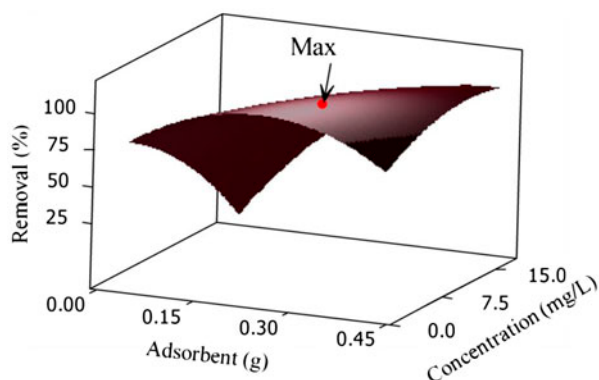The batch sorption experiments were carried out in 100-mL Erlenmeyer flasks, by contacting the solution

Fig. 1. Three-dimensional response surface.

with 0.100–0.300 g of the WC and 50-mL of the MB solutions (5–30 mg/L) at optimum pH. The Erlenmeyer flasks were subsequently agitated for up to 60 min at 300 rpm at room temperature until the equilibrium is reached. The MB concentration in the solution was measured using a double beam UV–vis spectrophotometer (jasco, Model UV–vis V-530, Japan) at 664 nm. The amount of adsorbed MB at equilibrium (q_e (mg/g)) was calculated using Eq. (3),

$$q_e = (C_0 - C_e)V/W \qquad (3)$$

where C_0 and C_e (mg/L) are the initial and equilibrium concentrations of liquid-phase dye, respectively. V (L) is the volume of the solution, and W (g) is the mass of dry adsorbent used.

The pH was adjusted by adding diluted NaOH (0.10 M) and/or HCl (0.10 M) before each experiment.

2.5. Adsorption kinetic studies

The effect of contact time for 50 mL of MB solution with concentration in the range of 5–15 mg/L was examined by agitating the solution by a magnetic stirrer at 300 rpm at room temperature. It was homogenously dispersed in solution. At a given time within the range of 0–60 min following the centrifugation for 5 min at 4,000 rpm, the phase separation occurred. Subsequently, the MB concentration was quantified and the actual amount of MB adsorbed at time t, (q_t (mg/g)), was calculated based on Eq. (4),

$$q_t = (C_0 - C_t)V/W \qquad (4)$$

where C_0 and C_t (mg/L) are the concentrations of MB at initial and at any time t, respectively. V (L) is the solution volume, and W (g) represents the mass of the adsorbent. The isotherm studies were performed by varying the initial MB concentration at various adsorbent dosages. At any condition, the amount of unadsorbed MB was determined and equilibrium value of adsorbed MB was evaluated using Eq. (4).

3. Results and discussion

3.1. Characterization of WC

3.1.1. FTIR

The characteristic functional groups of the adsorbent were investigated using FTIR spectra as the most powerful and well-stabilized instrument (see Fig. 3 for the FTIR of WC). Stretching vibration band around 1,700 cm^{-1} is assigned to carbonyl C=O group present
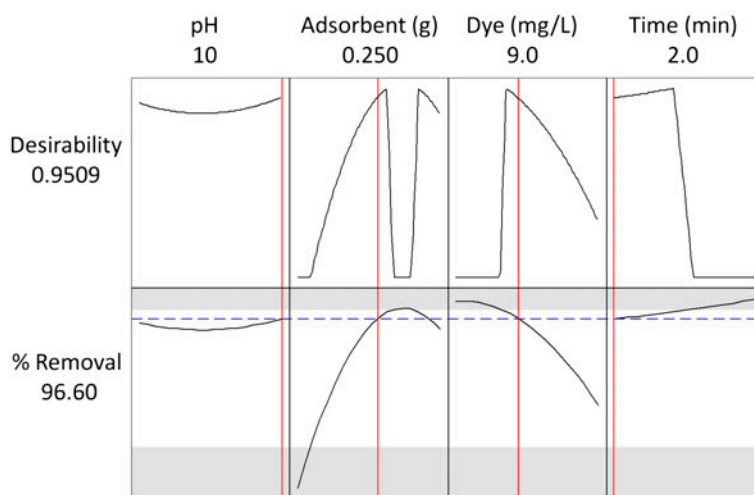

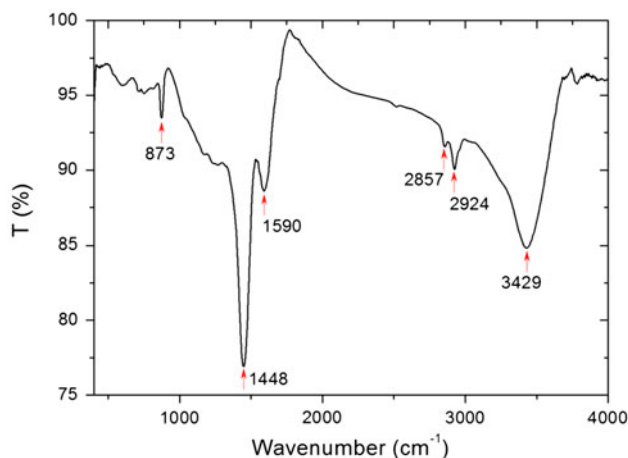Fig. 2. Optimization plot for the removal of MB by walnut carbon.

Fig. 3. FTIR spectrum of walnut carbon.

in aldehyde, ester, ketone, and acetyl derivatives. The strong band at 1,500 cm^{-1} may be due to C=C bond. The peaks appearing between 423 and 634 cm^{-1} are assigned to metal–oxygen (M–O) stretching mode in the structure of WC.

3.1.2. BET analysis of WC

Determination of iodine value is usually a complementary test to the N_2/77 K adsorption isotherms, which is assumed to measure the surface area in micropores within pore sizes of a material. Increase in four values of the adsorbent indicates a good and acceptable adsorption capacity of such an adsorbent [19]. Specific surface area (SSA) is an indication of the accessible area of adsorbent per unit mass and it generally depends on the surrounding phase that can modify the surface area. The interference of the surrounding phase is especially problematic for the Bruner–Emmet–Teller (BET) N_2 adsorption/desorption isotherm method, because the entire surface is modified by vacuum treatment before N_2 adsorption. Table 1 shows narrow microporosity structure of WC and its surface area, which is about 32.58 m^2/g. The total pore volume of WC was found to be 0.029 cm^3/g and its average pore diameter was found to be less than 10 nm. Total surface properties of the adsorbent are presented in Table 1.

3.1.3. pH$_{zpc}$

Characterization of the WC surface is governed by its ability for the adsorption of the target solute. Distribution of charge on the adsorbent surface plays a deep and appreciable role in the interaction of various

compounds with adsorbent and thus on the dye removal. The adsorbent charge may be either positive or negative. It may be greatly affected by the interaction of surface with solute ions. The adsorbent surface is neutral at a point known as zero point of charge (ZPC). At pH above this value (see Table 1), the surface becomes negatively charged, and the positive ions will be attracted on the surface due to electrostatic attraction. The negatively charged species will be accelerated at pH below the ZPC.

3.1.4. Determination of oxygen-containing functional groups

The type and concentration of the surface functional groups of WC were determined by the Boehm titration approach [20]. The surface titration method is based on a phenomenon in which only strong acidic carboxylic groups are neutralized by sodium bicarbonates (Na$_2$HCO$_3$), as well as lactonic and carboxylic groups are neutralized by sodium carbonate (Na$_2$CO$_3$). The weakly acidic phenolic groups are titrated via the addition of strong alkali, sodium hydroxide. The results of Boehm titration method for WC are presented in Table 1.

3.1.5. Kinetic study

Every adsorption process may follow either chemical reaction, diffusion control, and mass transfer or any combination of them. The investigation on the adsorption and the dye removal at various times allows evaluating the kinetic parameters and obtaining useful information to design and model the adsorption processes. This purpose was undertaken by evaluating the removal rate using various conventional models such as the Lagergren pseudo-first-order model (Eq. (5)) [21], the Ho's pseudo-second-order model (Eq. (6)) [22], and the Elovich model (Eq. (7)) [23].

$$q_t = q_e(1 - e^{-k_1 t}) \tag{5}$$

$$q_t = q_e^2 k_2 t / (1 + q_e k_2 t) \tag{6}$$

$$q_t = \frac{1}{\beta}\ln(t) + \frac{1}{\beta}\ln(\alpha\beta) \tag{7}$$

where q_e (mg/g) and q_t (mg/g) are the amounts of MB adsorbed at equilibrium and at time t, respectively. In addition, k_1 (min^{-1}) is the rate constant of pseudo-first-order adsorption, k_2 (g/mg min) is the rate constant of pseudo-second-order adsorption, α (mg/g min) is the initial adsorption rate, and β (g/mg) is the desorption

Table 3
Kinetic parameters of MB removal using 0.100 of WC for 5 mg/l of MB and 0.150 g of WC for 7.12, 10.00 and 15 mg/l of MB

Models	Parameters	0.100 g 5.00 mg/L	0.150 g		
			7.12 mg/L	10.00 mg/L	15.00 mg/L
First-order kinetic model:	K_1	0.032	0.044	0.014	0.016
$\log(q_e q_t) = \log(q_e) - (K_1/2.303)t$	q_e (cal)	0.729	0.455	1.288	1.824
	R^2	0.921	0.935	0.910	0.843
Second-order kinetic model:	K_2	0.241	0.537	0.255	0.148
$t/q_t = 1/k_2 q_e^2 + (1/q_e)t$	q_e (cal)	2.331	2.092	2.652	3.533
	R^2	0.996	0.999	0.998	0.990
	H	0.760	0.420	0.550	0.580
Intraparticle diffusion	K_{dif}	0.078	0.083	0.126	0.184
$q_t = K_{id} t_1/2 + C$	C	1.826	1.561	1.779	2.224
	R^2	0.744	0.899	0.957	0.851
Elovich	β	5.524	7.042	4.854	3.246
$q_t = 1/\beta \ln(\alpha\beta) + 1/\beta \ln(t)$	R^2	0.959	0.991	0.981	0.915
Experimental data	q_e (exp)	2.423	2.140	3.276	4.333

constant. The above-mentioned models were applied to fit the experimental kinetic data. The values of estimated parameters are shown in Tables 3 and 4. In spite of reasonable value of the R^2 corresponding to pseudo-first-order model at different amounts of adsorbent (R^2: 0.843–0.956), the experimental q_e values have great deviation from the theoretical values where this difference is even higher at large MB concentrations. Good and reasonable fit to Lagergren's model at low MB concentration does not hold at higher concentrations. However, the estimated q_e values of pseudo-second-order model accurately predict the adsorption kinetics over the entire working times. Therefore, this model satisfactorily predicts the kinetics of MB adsorption onto WC. The lack of fit of the Elovich model to the experimental data at low concentrations is improved at higher MB concentrations [24]. The initial adsorption rates can be calculated from the pseudo-second-order model by the following equation:

$$H = k_2 q_e^2 \qquad (8)$$

and the results are shown in Tables 3 and 4. The fact that the initial adsorption rate increases with increase in the initial MB concentration shows that the overall parameters of adsorption process are greatly influenced by the ratio of adsorbate to adsorbent. The value of initial sorption (H), which is proportional to the initial rate of adsorption, increases from 0.39 to 0.82 mg/(g min) with the increase in the initial MB concentration from 7.12 to 15.00 mg/L at 0.225 g of adsorbent. This value increases from 0.42 to 0.58 for

0.15 g and from 0.080 to 0.270 for 0.150 and 0.300 g of adsorbent, respectively.

The initial increase in H might be attributed to the enhancement in mass transport due to the driving force emerged from higher ratio of MB molecules to reactive vacant adsorbent sites. At higher concentrations, apparent MB dimerization [25] and difficult diffusion of large dimers in small adsorbent pores as well as possible electrostatic repulsion between MB molecules make the kinetic parameters worse.

Fig. 4 shows the linear plot of different kinetic models for the adsorption of different concentrations of MB onto 0.225 g of walnut carbon. The correlation coefficient (R^2) for the pseudo-second-order kinetic at different initial MB concentrations was found to be above 0.99. The calculated q_e values are in good agreement to the experimental values (Tables 3 and 4). For example, the equilibrium sorption capacity (q_e) increases from 1.536 to 2.762 mg/g by increasing the MB concentration from 7.12 to 15.00 mg/L at 0.225 g of adsorbent. The rate constant values decrease from 1.084 to 0.160 g/(mg.min) by increasing the initial MB concentration from 7.12 to 15.00 mg/L at 0.225 g of the adsorbent. The agreement between the experimental data and the model predicted values was expressed by the correlation coefficients (with R^2 values close or equal to 1). Among the pseudo-first- and second-order kinetic models, a critical factor for another judgment about their suitability is the agreement between the experimental and theoretical values. Comparison based on these two parameters shows the applicability of pseudo-second-order model for

Table 4
Kinetic parameters of MB removal using 0.225 and 0.300 g of WC for 7.12, 10.00, and 15 mg/l/l of MB.

| Models	Parameters	0.225 g			0.300 g		
		7.12 mg/L	10.00 mg/L	15.00 mg/L	7.12 mg/L	10.00 mg/L	15.00 mg/L
First-order kinetic model: $\log(q_e - q_t) = \log(q_e) - (K_1/2.303)t$	K_1	0.043	0.037	0.023	0.041	0.036	0.034
	q_e (cal)	0.234	0.453	1.250	0.056	0.136	0.399
	R^2	0.930	0.918	0.956	0.855	0.859	0.810
Second-order kinetic model: $t/q_t = 1/k_2 q_e^2 + (1/q_e)t$	K_2	1.084	0.480	0.160	9.681	2.253	0.680
	q_e (cal)	1.536	2.105	2.762	1.151	1.615	2.320
	R^2	0.999	0.999	0.994	1.000	1.000	0.999
	H	0.390	0.470	0.820	0.080	0.170	0.270
Intraparticle diffusion $q_t = K_{id}t_1/2 + C$	K_{dif}	0.038	0.076	0.152	0.010	0.025	0.078
	C	1.283	1.595	1.660	1.089	1.450	1.826
	R^2	0.835	0.939	0.966	0.833	0.826	0.774
Elovich $q_t = 1/\beta \ln(\alpha\beta) + 1/\beta \ln(t)$	β	14.705	7.751	4.000	71.428	22.222	7.143
	R^2	0.967	0.971	0.930	0.980	0.967	0.920
Experimental data	q_e (exp)	1.560	2.155	2.870	1.150	1.607	2.305
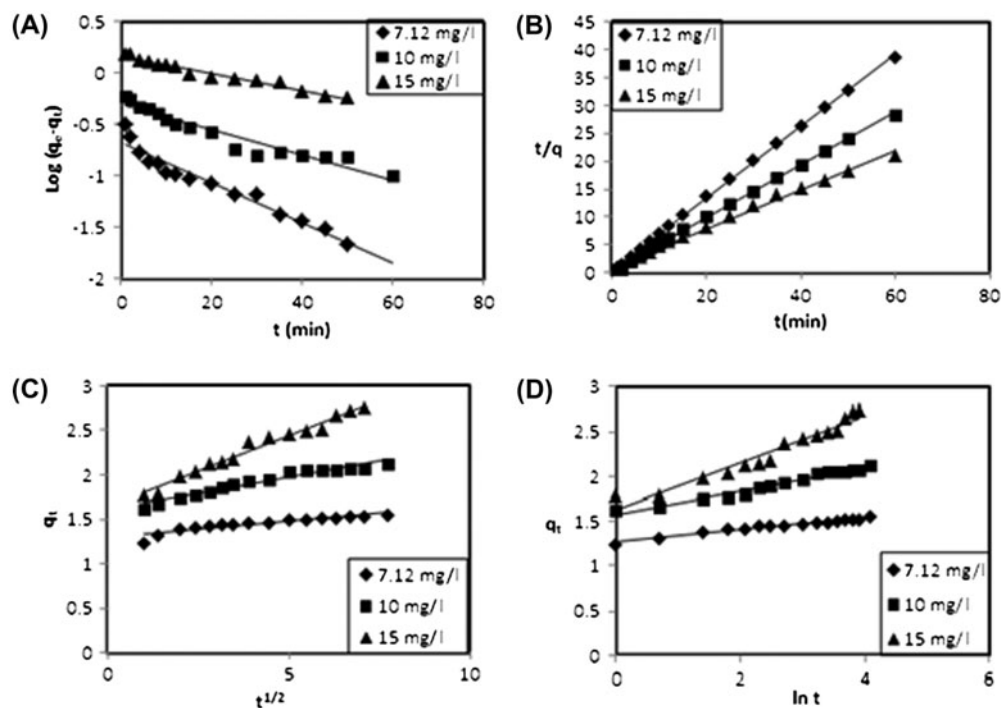
Fig. 4. Linear plot of different kinetic models at 0.225 g of walnut carbon and 7.12, 10.00, and 15.00 mg/L of methylene blue. (A) first-order kinetic model, (B) second-order kinetic model, (C) intraparticle diffusion model, and (D) Elovich model.

evaluating and fitting the experimental data over entire adsorption stage [26].

3.1.6. The intraparticle diffusion model

The initial dye concentration is not linearly related to the removal rate when pore diffusion is the predominant stage and limits the adsorption process. The MB transfer from bulk to the solid phase through intraparticle diffusion/transport process is known as rate-limiting step particularly in rapidly stirred batch process [23]. Therefore, the possible applicability of this model for the interpretation of experimental data was investigated according to its well-known equation:

$$q_t = K_{\text{dif}}t^{0.5} + C \tag{9}$$

where C (mg/g) is the intercept and k_{dif} (mg/g min$^{-1/2}$) is the intraparticle diffusion rate constant. The values of q_t were found to be linearly correlated to the values of $t^{1/2}$ (Fig. 4(C) for 0.225 g of WC). The rate constant k_{dif} is directly evaluated from the slope of the regression line (Tables 3 and 4). The C value (Tables 3 and 4) provides information about the thickness of boundary layer and external mass transfer resistance. As found, the constant C increases from 1.089 to 2.224 with increase in MB amount from 7.12 to 15 mg/L at 0.150–0.300 g of WC. It may be related to increase in thickness of the boundary layer and to decrease in the chance of the external mass transfer. Both of these behaviors support a prominent increase in the amount of internal mass transfer. The high value of R^2 shows suitability of this model to explain the experimental data. This may confirm that the rate-limiting step is the intraparticle diffusion process. The intraparticle diffusion rate constant (k_{dif}) value was in the range of 0.038–0.152 mg/g min$^{-1/2}$ at 0.225 g of adsorbent with a good positive correlation between the initial dye concentration and this linear relationship, which shows high contribution of intraparticle diffusion on the adsorption process. Generally, in kinetic studies, passing the plot of intraparticle diffusion through origin shows that this mechanism solely limits the adsorption rate. This situation was not achieved in our study, which shows that another alternative model in addition to intraparticle diffusion model is required to follow the adsorption data.

3.1.7. Equilibrium isotherms

Adsorption equilibrium isotherm is designed based on the mathematical relation between the amounts of

target adsorbed per gram of adsorbent (q_e (mg/g)) to the equilibrium unadsorbed amount of dye in the solution (C_e (mg/L)) at constant temperature. Isotherm study is of high theoretical and practical interests to obtain knowledge about the surface properties of adsorbent and removal mechanism [27].

3.1.8. Langmuir isotherm

The Langmuir isotherm is valid for the adsorption of solute from liquid solution on finite number of similar and equi-energy surface sites, without transmigration of adsorbate in the surface plane [3]. The maximum adsorption capacity corresponding to complete monolayer coverage on the adsorbent surface is calculated by the following well-known procedure. A plot of C_e/Q_e vs. C_e at various amounts of WC such as 0.150, 0.225, and 0.300 g, which is generally a straight line with a slope of $1/Q_m$ and an intercept of $1/(k_aQ_m)$, is shown in Fig. 5(A). At various amounts of WC, this line is used to calculate the respective constant present in this model (Table 5). The high correlation coefficients and high maximum monolayer capacity (3.745–4.739 mg/g using 0.15–0.3 g

of adsorbent) show strong positive evidence on the usefulness of the Langmuir model, accurately, and predict the properties of adsorption process (Table 5).

The separation factor (RL) is calculated to evaluate the adsorption capacity [28].

$$RL = 1/(1 + K_aC_0) \tag{10}$$

where K_a(L/mg) is the Langmuir constant and C_0 (mg/L) is the initial concentration. The adsorption process can be determined as favorable when the RL value is between 0 and 1. It was found that the RL values at all conditions are lower than 1. This strongly supports the favorable adsorption and shows a good fit to the Langmuir model for the experimental data. In addition, increase in the RL value with increasing initial MB concentration and adsorbent dosage shows high tendency of MB for the adsorption onto WC.

3.1.9. Freundlich isotherm

The Freundlich isotherm model [29] is applicable for non-ideal heterogeneous sorption with the logarithmic decrease in the enthalpy of adsorption and with
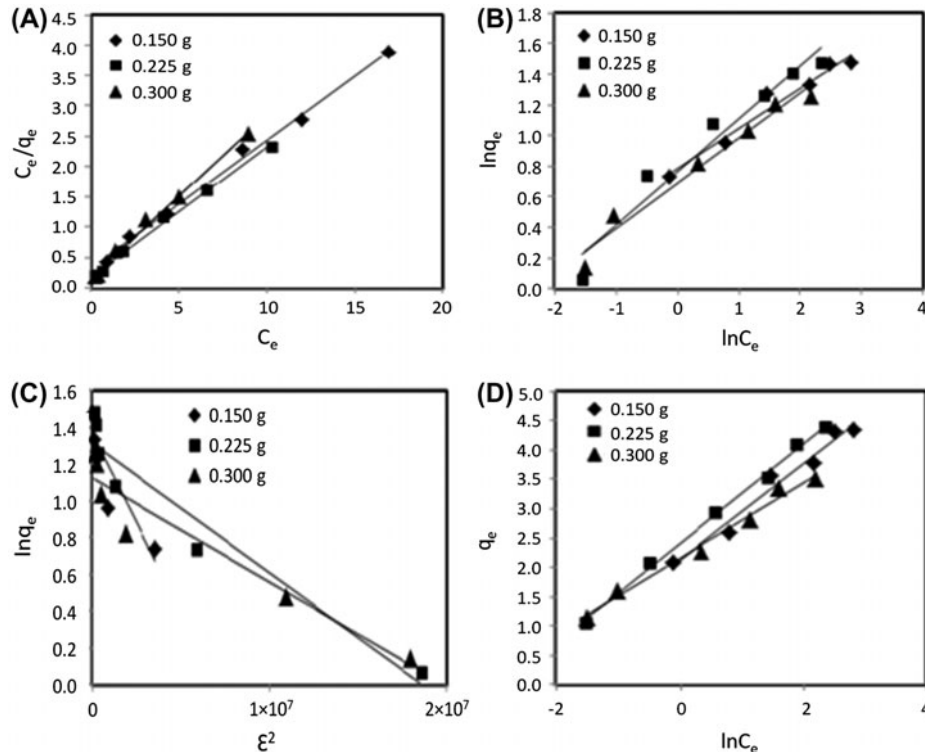

Fig. 5. Linear Plot of different isotherm models in 0.150, 0.225, and 0.300 g of walnut carbon and MB concentration ranged 5–30 mg/L. (A) Langmuir isotherm, (B) Freundlich isotherm, (C) Dubinin–Radushkevich isotherm, and (D) Tempkin isotherm.

Table 5
Comparison of the different isotherm parameters for MB adsorption on 0.150, 0.225, and 0.300 g of walnut carbon

Isotherms	Parameters	Adsorbent (g)		
		0.150 g	0.225 g	0.300 g
Langmuir	Q_m (mg g^{-1})	4.739	4.716	3.745
$C_e/q_e = 1/K_aQ_m + C_e/Q_m$	K_a (L mg^{-1})	0.659	1.065	1.467
	RL	0.048–0.175	0.030–0.158	0.022–0.087
	X^2	0.634	1.137	1.039
	R^2	0.995	0.995	0.995
Freundlich	$1/n$	0.260	0.349	0.293
$\ln q_e = \ln KF + (1/n)\ln C_e$	K_F (L mg^{-1})	2.196	2.144	1.950
	X^2	2.852	2.732	1.571
	R^2	0.963	0.949	0.971
Tempkin	B_1	0.815	0.848	0.638
$q_e = B_l \ln KT + B_l \ln C_e$	K_T (L mg^{-1})	13.968	17.579	29.488
	X^2	3.423	4.142	5.050
	R^2	0.968	0.996	0.987
Dubinin and Radushkevich	Q_s (mg g^{-1})	3.892	3.709	3.055
$\ln q_e = \ln Q_s - K\varepsilon^2$	$K(10^{-8})$	20	7	6
	E (kJ/mol) $= 1/(2\,K)^{1/2}$	1,581.139	2,672.612	2,886.751
	X^2	0.361	0.789	0.717
	R^2	0.802	0.934	0.923

increase in the fraction of occupied sites. K_f values are a criterion of the bonding energy and adsorption or distribution coefficient indicating the amount of target compound adsorbed onto adsorbent until the equilibrium is achieved. $1/n$ shows adsorption intensity and surface heterogeneity. The value approaches zero by increasing the heterogeneous nature of the surface. The $1/n$ value less than 1 indicates normal Langmuir isotherm, while $1/n$ above 1 indicates bimechanism and cooperative adsorption. The applicability of the Freundlich adsorption isotherm was assessed by plotting $\ln q_e$ vs. $\ln C_e$ (Fig. 5(B)). The values for the constants in the model at various amounts of adsorbent are shown in Table 5. The correlation coefficients (0.96–0.97) and higher error value of this model show that the Freundlich model has lower efficiency compared to the Langmuir model.

3.1.10. Tempkin isotherm

R^2 value shows the applicability of each model for the explanation of the experimental data and the lower value concerns to error analysis. Both Langmuir and Freundlich models have reasonable and acceptable R^2 value. However, conventional model, such as Tempkin isotherm, (Fig. 5(C)) has commonly been applied in the following linear form [25]:

$$q_e = \beta \ln \alpha + \beta \ln C_e \qquad (11)$$

where $\beta = (RT)/b$ is related to the heat of adsorption, T is the absolute temperature in Kelvin, and R (8.314 J mol^{-1} K^{-1}) is the universal gas constant [30]. The evaluation and assessment of the experimental equilibrium adsorption data show the usability of this model for the explanation of adsorption. The linear isotherm constants and coefficients of determination are presented in Table 5. The heat of MB adsorption onto WC was found to be increased from 0.638 to 0.815 kJ mol^{-1} with a decrease in WC dosage from 0.3 to 0.15 g. The correlation coefficient (R^2) obtained from Tempkin model is comparable with that obtained from Langmuir and Freundlich equations. According to χ, as a significant criterion, best applicable model is the Langmuir model.

3.1.11. Dubinin–Radushkevich (D–R) isotherm

The D–R model was applied to estimate the porosity, free energy, and the characteristics of adsorbents [31]. The D–R isotherm (Fig. 5(D)) is applicable to homogeneous surfaces. Constant adsorption potential is calculated from the following linear equation.

$$\ln q_e = \ln Q_m - B\varepsilon^2 \qquad (12)$$

where B is a constant related to the adsorption energy, Q_m is theoretical saturation capacity, and ε is
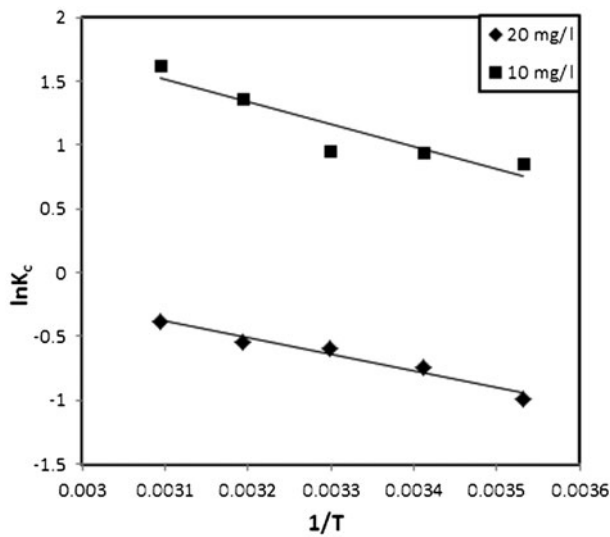
Fig. 6. Plot of lnK$_c$ vs. 1/T for the estimation of thermodynamic parameters.

the Polanyi potential which is generally calculated from Eq. (13).

$$\varepsilon = RT \ln(1 + 1/C_e) \tag{13}$$

The slope of the plot of lnq_e vs. ε gives B (mol^2/(kJ^2)) and the intercept yields the adsorption capacity,

(Q_m (mg/g)). The mean free energy of adsorption (E), which concerns to energy transport from target molecule to the adsorbent surface, is generally evaluated using the following equation [32]:

$$E = (2B)^{-1/2} \tag{14}$$

The calculated values of D–R parameters (Table 5) show that the saturation adsorption capacity at different amounts of the adsorbent is in the range of 3.055–3.892, and is in good agreement with respective Langmuir value. The values of E, obtained from Eq. (14), are in the range of 1,581.139–2,886.751 mol^{-1}. This strongly shows that physisorption process plays a significant contribution in the adsorption of MB onto WC. Another important criterion for evaluating the applicability of each model was applied using a non-linear chi-square statistical test (χ^2) [33]:

$$\chi^2 = \text{Sum} (q_{e,\exp} - q_{e,\text{cal}}/q_{e,\text{cal}})^2 \tag{15}$$

where $q_{e,\exp}$ and $q_{e,\text{cal}}$ are the experimental and calculated adsorption capacities, respectively. Good agreement between the data acquired by each model to the experimental data makes it possible to lower χ^2 value and increase the applicability of each model and vice versa. The higher R^2 value and smaller χ^2 value

Table 6
Thermodynamic data for adsorption of methylene blue by 0.225 g of walnut carbon

Concentration	Parameter							
	ΔG at $T(°K) = 283$	ΔG at $T(°K) = 293$	ΔG at $T(°K) = 303$	ΔG at $T(°K) = 313$	ΔG at $T(°K) = 323$	ΔH	ΔS	R^2
10.00 mg/L	−1,773.000	−2,353.000	−2,933.000	−3,512.900	−4,092.900	14,649.270	58.000	0.844
20.00 mg/L	2,211.100	1,960.900	1,602.700	1,298.500	994.300	10,824.830	30.420	0.964

Table 7
Maximum monolayer sorption of several adsorbents

Sorbent	Sorption capacity (mg g−1)	Reference
Activated carbon (coconut shell fibbers)	19.59	[35]
Activated carbon (olive stones)	303	[36]
Cotton waste	240	[37]
Date pits	80.3	[38]
Fly ash	53.84	[39]
Perlite	5.6–9.08	[40]
Perlite	162.3	[41]
Perlite (EP)	17.4–31.7	[42]
Pyrophyllite	70.42	[43]
Zeolite	53.1	[41]
Homemade walnut carbon	3.74–4.74	This study

for Langmuir isotherm in comparison with other models show its superiority to other model for the explanation of the experimental equilibrium data. The lower correlation coefficient (R^2) of Freundlich model in comparison to Langmuir model suggests that the removal process is well modeled by monolayer compared to multilayer adsorption.

3.1.12. Adsorption thermodynamics

Thermodynamic parameters for adsorption of MB onto WC were obtained at various temperatures of 10, 20, 30, 40, and 50°C. This was performed to investigate the spontaneous nature of the adsorption process. The equation used is expressed as:

$$\Delta G = -RT \ln K_e \tag{16}$$

A plot of $\ln K_e$ against $1/T$ gives a graph (Fig. 6), from the slope of which ΔG can be obtained. Thermodynamic parameter results for the adsorption of MB onto WC at various temperatures are reported in Table 6. The adsorption process was found to be spontaneous in nature for the case 10 mg/L with negative values of change of Gibbs free energy (ΔG). For the case 20 mg/L, the positive values of the change of Gibbs free energy indicate that the process is non-spontaneous. The positive values of both enthalpy (ΔH) and entropy (ΔS) obtained for the MB adsorption onto WC showed that the adsorption processes are endothermic with random characteristics. The absolute value of change of Gibbs free energy for physical adsorption (–20 to 0 kJ/mol) is smaller than that of chemisorptions (–80 to –400 kJ/mol) [34]. The results obtained from this study for Gibbs free energy prove that the adsorption processes are physical in nature.

3.1.13. Comparison of other adsorbents for the MB removal

Advantages of these adsorbents include: ease of production, low cost, abundance of raw materials, the use of green chemistry, and reusability after heating. Therefore, it could be used as a good adsorbent for the removal of water pollution. Maximal adsorption capacities of several adsorbents [35–43] are given in Table 7.

4. Conclusion

This investigation showed the applicability of WC as a good, green, low-cost, and locally available adsorbent for the removal of MB from aqueous solutions in a very short time (2 min). By using RSM, the optimum values of the pH, adsorbent dosage, MB concentration, and contact time were found to be 10, 0.250 g, 9.00 mg/L, and 2 min, respectively, with the MB removal percentage above 95%. Langmuir isotherm gave a best fit to adsorption data. This fact may be attributed to high Langmuir surface area of the adsorbent. The data indicated that the adsorption kinetics follow the pseudo-second-order rate in addition to intraparticle diffusion. It was concluded that the WC could be employed as a low-cost adsorbent and it could be a good alternative to commercial activated carbon for the removal of dyes from wastewater. Further studies on quantitative characterization of this adsorbent and mechanisms involved are needed. It is also suggested to investigate the applicability of this adsorbent for the removal of other dyes as well as its possible industrial application.

List of symbols

x_i, x_j	—	coded values of the factors
b_0, b_i, b_{ii}, and b_{ij}	—	constant, linear, quadratic, and interaction coefficients, respectively
x_2, x_3, x_2^2, x_3^2, and $x_2 x_3$	—	amount of adsorbent, dye concentration, square of amount of adsorbent, square of dye concentration, as well as the interaction of the amount of adsorbent and dye concentration, respectively
C_0 and C_e (mg/L)	—	initial and equilibrium concentrations of liquid-phase dye, respectively
V (L)	—	volume of the solution
W (g)	—	mass of dry adsorbent used
C_t (mg/L)	—	concentration of MB at any time t
q_e (mg/g) and q_t (mg/g)	—	amounts of MB adsorbed at equilibrium and at time t, respectively
k_1 (min^{-1})	—	rate constant of pseudo-first-order adsorption
k_2 (g/mg min)	—	rate constant of pseudo-second-order adsorption
α (mg/g min)	—	initial adsorption rate
β (g/mg)	—	desorption constant
H	—	initial sorption
k_{dif} (mg/g min$^{-1/2}$)	—	intraparticle diffusion rate constant
RL	—	separation factor
K_a (L/mg)	—	Langmuir constant

$T(K)$	—	absolute temperature
R (8.314 J mol^{-1} K^{-1})	—	universal gas constant
B	—	constant related to the adsorption energy
Q_m	—	theoretical saturation capacity
ε	—	Polanyi potential
E	—	mean free energy of adsorption
χ^2	—	chi-square
$q_{e,\exp}$ and $q_{e,\text{cal}}$	—	experimental and calculated adsorption capacity values, respectively
ΔG	—	Gibbs free energy
ΔH	—	enthalpy
ΔS	—	entropy

References

[1] G. CRINI, Non-conventional low-cost adsorbents for dye removal: A review, Bioresour. Technol. 97 (2006) 1061–1085.

[2] G. Mishra, M. Tripathy, A critical review of the treatment for decolourization of textile effluent, Colourage 40 (1993) 35–38.

[3] M. Ghaedi, Comparison of cadmium hydroxide nano-wires and silver nanoparticles loaded on activated carbon as new adsorbents for efficient removal of Sunset yellow: Kinetics and equilibrium study, Spectrochim. Acta A. 94 (2012) 346–351.

[4] M. Ghaedi, S. Heidarpour, S. Nasiri, S. Kokhdan, R. Sahraie, A. Daneshfar, B. Brazesh, Comparison of silver and palladium nanoparticles loaded on activated carbon for efficient removal of Methylene blue: Kinetic and isotherm study of removal process, Powder Technol. 228 (2012) 18–25.

[5] T. Robinson, G. McMullan, R. Marchant, P. Nigam, Remediation of dyes in textile effluent: A critical review on current treatment technologies with a proposed alternative, Bioresour. Technol. 77 (2001) 247–255.

[6] O. Ozdemir, M. Turan, A. Turan, A. Faki, A.B. Engin, Feasibility analysis of color removal from textile dyeing wastewater in a fixed-bed column system by surfactant-modified zeolite, J. Hazard. Mater. 166 (2009) 647–654.

[7] R.P. Han, J.H. Zhang, W.H. Zou, J. Shi, H.M. Liu, Equilibrium biosorption isotherm for lead ion on chaff, J. Hazard. Mater. 125 (2005) 266–271.

[8] V.K. Gupta, I. Ali, D. Suhas, Equilibrium uptake and sorption dynamics for the removal of a basic dye (basic red) using low cost adsorbents, J. Colloid Interface Sci. 265 (2003) 257–264.

[9] Y.S. Ho, W.T. Chiu, C.C. Wang, Regression analysis for the sorption isotherms of basic dyes on sugarcane dust, Bioresour. Technol. 96 (2005) 1285–1291.

[10] K.V. Kumar, Comparative analysis of linear and non-linear method of estimating the sorption isotherm parameters for malachite green onto activated carbon, J. Hazard. Mater. 136 (2006) 197–202.

[11] M. Ghaedi, S. Hajati, B. Barazesh, F. Karimi, G. Ghezelbash, Saccharomyces cerevisiae for the biosorption of basic dyes from binary component systems and the high order derivative spectrophotometric method for simultaneous analysis of Brilliant green and Methylene blue, J. Ind. Eng. Chem. 19 (2013) 227–233.

[12] M. Ghaedi, S. Hajati, F. Karimi, B. Barazesh, G. Ghezelbash, Equilibrium, kinetic and isotherm of some metal ion biosorption, J. Ind. Eng. Chem. 19 (2013) 987–992.

[13] Y.S. Ho, Second-order kinetic model for the sorption of cadmium onto tree fern: A comparison of linear and non-linear methods, Water Res. 40 (2007) 119–125.

[14] R. Dolphen, N. Sakkayanwong, P. Thiravetyan, W. Nakbanpote, Adsorption of Reactive Red 141 from wastewater onto modified chitin, J. Hazard. Mater. 145 (2007) 250–255.

[15] C. Kannan, T. Sundaram, T. Palvannan, Environmentally stable adsorbent of tetrahedral silica and non-tetrahedral alumina for removal and recovery of malachite green dye from aqueous solution, J. Hazard. Mater. 157 (2008) 137–145.

[16] S.J. Culp, L.R. Blankenship, D.F. Kusewitt, D.R. Doerge, L.T. Mulligan, F.A. Beland, Toxicity and metabolism of malachite green and leucomalachite green during short-term feeding to Fischer 344 rats and B6C3F1 mice, Chem. Biol. Interact. 122 (1999) 153–170.

[17] M. Kandah, R. Shawabkeh, M. Al-Zboon, Synthesis and characterization of activated carbon from asphalt, Appl. Surf. Sci. 253 (2006) 821–826.

[18] O.A. Ekpete, M.J.N. Horsfall, Preparation and characterization of activated carbon derived from fluted pumpkin stem waste (*Telfairiaoccidentalis* Hook F), Res. J. Chem. Sci. 1 (2011) 10–17.

[19] S.D. Khattri, M.K. Singh, Adsorption of basic dyes from aqueous solution by natural adsorbent, Indian J. Chem. Technol. 6 (1999) 112–116.

[20] I.I. Salame, T.J. Bandosz, Surface chemistry of activated carbons: Combining the results of temperature-programmed desorption, boehm, and potentiometric titrations, J. Coll. Int. Sci. 240 (2001) 252–258.

[21] Y.S. Ho, A.E. Ofomaja, Kinetics and thermodynamics of lead ion sorption on palm kernel fibre from aqueous solution, Process Biochem. 40 (2005) 3455–3461.

[22] S. Kundu, A.K. Gupta, Investigation on the adsorption efficiency of iron oxide coated cement (IOCC) towards As(V) kinetics, equilibrium and thermodynamic studies, Colloid Surface A. 273 (2006) 121–128.

[23] S. Lagergren, Zurtheorie der sogenannten adsorption gelösterstoffe (About the theory of so-called adsorption of soluble substances), Kungliga Svenska Vetenskapsakademiens, Handlingar 24 (1898) 1–39.

[24] Y.S. Ho, G. McKay, The kinetics of sorption of divalent metal ions onto sphagnum moss peat, Water Res. 34 (2000) 735–742.

[25] H.M.F. Freundlich, Uber die adsorption in losungen (Over the adsorption in solution), Z. Phys. Chem. 57 (1906) 385–470.

[26] M. Ghaedi, B. Sadeghian, A.A. Pebdani, R. Sahraei, A. Daneshfar, C. Duran, Kinetics, thermodynamics and equilibrium evaluation of direct yellow 12 removal by adsorption onto silver nanoparticles loaded activated carbon, Chem. Eng. J. 187 (2012) 133–141.

[27] Z. Jiang, Y. Liu, X. Sun, F. Tian, F. Sun, C. Liang, W. You, C. Han, C. Li, Activated carbons chemically modified by concentrated H$_2$SO$_4$ for the adsorption of pollutants from wastewater and dibenzothiophene from fuel oils, Langmuir 19 (2003) 731–736.

[28] M. Dogan, M. Alkan, Y. Onganer, Adsorption of methylene blue from aqueous solution onto perlite, Water, Air, Soil Pollut. 120 (2000) 229–249.

[29] V.K. Garg, R. Kumar, R. Gupta, Removal of malachite green dye from aqueous solution by adsorption using agro-industry waste: A case study of Prosopis cineraria, Dyes Pigm. 62 (2004) 1–10.

[30] G. Akkaya, A. Ozer, Adsorption of acid red 274 (AR 274) on Dicranellavaria: Determination of equilibrium and kinetic model parameters, Process Biochem. 40 (2005) 3559–3568.

[31] M.M. Dubinin, The potential theory of adsorption of gases and vapors for adsorbents with energetically non-uniform surface, Chem. Res. 60 (1960) 235–266.

[32] M.M. Dubinin, Modern state of the theory of volume filling of micropore adsorbents during adsorption of gases and steams on carbon adsorbent, Zh. Fiz. Khim. 39 (1965) 1305–1317.

[33] L.V. Radushkevich, Potential theory of sorption and structure of carbons, Zh. Fiz. Khim. 23 (1949) 1410–1420.

[34] Q. Li, Q. Yue, Y. Su, B. Gao, H. Sun, Equilibrium, thermodynamics and process design to minimize adsorbent amount for the adsorption of acid dyes onto cationic polymer-loaded bentonite, Chem. Eng. J. 158 (2010) 489–497.

[35] G.T. Faust, J.C. Hathaway, G. Millot, A restudy of steven site and allied minerals, Am. Miner. 44 (1959) 342–370.

[36] E. Voudrias, K. Fytianos, E. Bozani, Sorption–desorption isotherms of dyes from aqueous solutions and wastewaters with different sorbent materials, Global Nest: the Int. J. 4 (2002) 75–83.

[37] T.W. Weber, R.K. Chackravorti, Pore and solid diffusion models for fixed bed adsorbers, Amer. Inst. Chem. Eng. J. 20 (1974) 228–238.

[38] D. Suteu, D. Bilba, Equilibrium and kinetic study of reactive dye brilliant red HE-3B adsorption by activated charcoal, Acta. Chim. Slov. 52 (2005) 73–79.

[39] A.S. Ozcan, B. Erdem, A. Ozcan, Adsorption of Acid Blue 193 from aqueous solutions onto Na-bentonite and DTMA-bentonite, J. Coll. Inter. Sci. 280 (2004) 44–54.

[40] E. Erdem, G. Colgecen, R. Donat, The removal of textile dyes by diatomite, earth, J. Coll. Inter. Sci. 282 (2005) 314–319.

[41] R.J. Stephenson, J.B. Sheldon, Coagulation and precipitation of a mechanical pulping effluent: 1. Removal of carbon and turbidity, Water Res. 30 (1996) 781–792.

[42] G.M. Walker, L.R. Weatherley, Fixed bed adsorption of acid dyes onto activated carbon, Environ. Pollut. 99 (1998) 133–136.

[43] Y. Al-Degs, M.A.M. Kharaisheh, S.J. Allen, M.N. Ahmad, Effect of carbon surface chemistry on the removal of reactive dyes from textile effluent, Water Res. 34 (2000) 927–935.